

# Time-scale of breakup of the halo nucleus $^{11}\text{Be}$

P. Banerjee

*Theory Group, Saha Institute of Nuclear Physics,  
1/AF Bidhan Nagar, Calcutta - 700 064, INDIA*

(October 11, 2018)

## Abstract

We investigate the post-acceleration of the  $^{10}\text{Be}$  fragment in Coulomb breakup reaction of the halo nucleus  $^{11}\text{Be}$ , assuming that the excitation of the projectile is to states in the low energy continuum. The method used retains all finite-range effects associated with the interactions between the breakup fragments and can use realistic wave functions for the halo nuclei. We apply the method to compute the average momenta of the  $^{10}\text{Be}$  fragment at four different scattering angles following breakup of  $^{11}\text{Be}$  on a Au target at 42 MeV/nucleon beam energy. Our results, which are in qualitative agreement with recent precision experimental data, are consistent with the picture of no post-acceleration effect. The implication is that the breakup takes place on a time-scale long compared to the collision time.

PACS numbers: 24.10.Eq, 25.60.-t, 25.70.Mn

arXiv:nucl-th/9812040v1 16 Dec 1998

In the breakup reaction of a halo nucleus, there could be a difference in the velocity of the charged breakup fragment in the final channel and the beam velocity. The magnitude of this velocity difference can be used as a probe to measure the time-scale of such reactions [1]. If the breakup takes place at or around the distance of closest approach, the charged fragment, which is lighter than the projectile, is accelerated more on the way out than the projectile was decelerated on the way in. This phenomenon is often referred to as “post-acceleration”. On the other hand, if the breakup occurs long after the fragment has left the strong Coulomb field near the target, the deceleration and acceleration would be the same. Then the fragment velocity would be equal to the beam velocity.

The subject of post-acceleration of the heavy charged core in the breakup of halo nuclei on heavy targets has been a controversial issue [2]. Recent measurements on Coulomb dissociation of  $^{11}\text{Li}$  and  $^{11}\text{Be}$  on heavy targets reveal post-acceleration of the charged cores [3–5]. In the measurement of breakup of  $^{11}\text{Li}$  on Pb target at MSU, a clear non-zero velocity difference between  $^9\text{Li}$  and the two neutrons has been seen [3]. However, this difference has not been observed clearly when the velocities of the  $^{10}\text{Be}$  fragment and the neutron in the final channel have been measured by Nakamura *et al.* at RIKEN, Japan in the breakup of  $^{11}\text{Be}$  on Pb at 72 MeV/nucleon [4]. But significant post-acceleration has been reported by them when the mean longitudinal momentum of  $^{10}\text{Be}$  has been measured as a function of its scattering angle. Measurements done at MSU on the average parallel momentum of  $^9\text{Li}$  (resulting from breakup of  $^{11}\text{Li}$  on U) as a function of its scattering angle have similar conclusions regarding post-acceleration of this breakup fragment [5]. Anne *et al.* have found little post-acceleration in their measurements of the neutron momentum distribution from the fragmentation of  $^{11}\text{Be}$  at GANIL [6]. It has been argued by them that the post-acceleration effects in these reactions should be small because the collision time is much less than the characteristic time for the disintegration of the halo.

Theoretically, there have been numerous attempts to calculate the post-acceleration of charged fragments in breakup reactions induced by halo nuclei. The observations of Nakamura *et al.* agree with the classical calculation of Baur, Bertulani and Kalassa [7], where the concept of a ‘classical breakup radius’ has been introduced. But the result of this calculation does not agree with the angular dependence of the  $^9\text{Li}$  momentum centroid as observed in the MSU experiment [5]. This calculation is also in contradiction with the time-dependent, three dimensional Schrödinger calculation of Kido, Yabana and Suzuki [8]. The three dimensional quantum mechanical calculations of these higher order Coulomb final state effects by Esbensen, Bertsch and Bertulani [1] do not support the argument of Anne *et al.* [6]. However, post-acceleration effects noticed in the energy distributions of charged breakup fragments calculated at different angles within the theory of post form DWBA Coulomb breakup are insignificant [2,9]. There the authors are of opinion that the breakup takes place at large distances because of the small separation energy of the valence neutron(s). Thereby the effect of repulsion of the strong Coulomb field is reduced, producing no appreciable post-acceleration [2,9]. No post-acceleration has also been observed in the parallel momentum distribution of  $^{10}\text{Be}$  resulting from calculations using an adiabatic model of Coulomb breakup of  $^{11}\text{Be}$  on heavy (U and Ta) targets [10]. Thus, different observables have been calculated in this regard with different conclusions and theoretically also the observation of post-acceleration remains debatable.

In order to verify the experimental result of Nakamura *et al.*, precise measurements have

been done very recently at MSU [11]. In this brief report, we calculate the post-acceleration of the charged fragment  $^{10}\text{Be}$  in the Coulomb dissociation of the halo nucleus  $^{11}\text{Be}$  and compare with the MSU data. We follow the theoretical formalism which was first described in [12] for the Coulomb breakup of a light weakly bound two-body composite nucleus  $a$  consisting of a charged core  $c$  and a neutral valence particle  $v$  on target  $t$  at energies of a few tens of MeV per nucleon and above. There are two approximations used in this theory - that the dominant projectile breakup configurations excited are in the low-energy continuum and that the valence particle does not interact with the target. The theory is fully quantum mechanical and is also non-perturbative. The method retains all finite-range effects associated with the interactions among the breakup fragments and includes the initial and final state interactions to all orders. It allows the use of realistic wave functions to describe the halo nuclei.

The transition amplitude for the above elastic Coulomb breakup reaction, in the c.m. frame, is given by (Fig. 1)

$$T_{\sigma_c\sigma_v;\sigma_a} = \langle \chi^{(-)}(\mathbf{k}_c, \mathbf{R}_c) \mathcal{S}_{\sigma_c} e^{i\mathbf{k}_v \cdot \mathbf{R}_v} \mathcal{S}_{\sigma_v} | V_{cv} | \Psi_{\mathbf{k}_a\sigma_a}^{(+)}(\mathbf{r}, \mathbf{R}) \rangle, \quad (1)$$

where  $\mathcal{S}_{\sigma_c}$  and  $\mathcal{S}_{\sigma_v}$  are the core and valence particle internal wavefunctions with  $\sigma_c$  and  $\sigma_v$  their spin projections.  $\hbar\mathbf{k}_c$  and  $\hbar\mathbf{k}_v$  are the asymptotic momenta of these fragments, conjugate to  $\mathbf{R}_c$  and  $\mathbf{R}_v$ , respectively, and  $\chi^{(-)}$  is an in-going waves Coulomb distorted wave function describing the  $c$ - $t$  relative motion in the final state. Since it is assumed that  $V_{vt} = 0$  the valence particle is described by a plane wave in the final state.

Following the adiabatic approximation of ref. [13], the exact three-body scattering wave function  $\Psi_{\mathbf{k}_a\sigma_a}^{(+)}(\mathbf{r}, \mathbf{R})$  separates in the variables  $\mathbf{R}_c$  and  $\mathbf{r}$ , namely

$$\Psi_{\mathbf{k}_a\sigma_a}^{(+)}(\mathbf{r}, \mathbf{R}) \approx \Psi_{\mathbf{k}_a\sigma_a}^{\text{AD}}(\mathbf{r}, \mathbf{R}) = \Phi_{a\sigma_a}(\mathbf{r}) e^{i\gamma\mathbf{k}_a \cdot \mathbf{r}} \chi^{(+)}(\mathbf{k}_a, \mathbf{R}_c). \quad (2)$$

Here  $\chi^{(+)}$  is a Coulomb distorted wave representing projectile's motion in the incident channel, evaluated at the core coordinate  $\mathbf{R}_c$  and  $\gamma = m_v/(m_c + m_v)$ .

The projectile ground state wave function is given by

$$\Phi_{a\sigma_a}(\mathbf{r}) = \sum_{l\mu jm\sigma'_c\sigma'_v} \langle s_c\sigma'_c jm | s_a\sigma_a \rangle \langle l\mu s_v\sigma'_v | jm \rangle \Phi_a^{l\mu}(\mathbf{r}) \mathcal{S}_{\sigma'_c} \mathcal{S}_{\sigma'_v}, \quad (3)$$

where  $\Phi_a^{l\mu}(\mathbf{r}) = i^l u_l(r) Y_{l\mu}(\hat{\mathbf{r}})$ , the  $u_l$  are radial wavefunctions, and the  $Y_{l\mu}$  are the spherical harmonics. Since the only distorting interaction  $V_{ct}$  is assumed to be central, the integrations over spin variables can be carried out in Eq. (1). The required approximate transition amplitude can then be expressed as

$$T_{\sigma_c\sigma_v;\sigma_a}^{\text{AD}} = \sum_{l\mu jm} \langle s_c\sigma_c jm | s_a\sigma_a \rangle \langle l\mu s_v\sigma_v | jm \rangle \beta_{l\mu}^{\text{AD}}, \quad (4)$$

where the reduced transition amplitude  $\beta_{l\mu}^{\text{AD}}$  is

$$\beta_{l\mu}^{\text{AD}} = \langle \chi^{(-)}(\mathbf{k}_c, \mathbf{R}_c) e^{i\mathbf{k}_v \cdot \mathbf{R}_v} | V_{cv} | \Phi_a^{l\mu}(\mathbf{r}) e^{i\gamma\mathbf{k}_a \cdot \mathbf{r}} \chi^{(+)}(\mathbf{k}_a, \mathbf{R}_c) \rangle. \quad (5)$$

Since  $\mathbf{R}_v = \alpha \mathbf{R}_c + \mathbf{r}$  (Fig. 1), where  $\alpha = m_t/(m_t + m_c)$ , then without further approximation the entire adiabatic amplitude now separates exactly in the coordinates  $\mathbf{R}_c$  and  $\mathbf{r}$ , as

$$\begin{aligned} \beta_{l\mu}^{\text{AD}} &= \langle e^{i\mathbf{q}_v \cdot \mathbf{r}} | V_{cv} | \Phi_a^{l\mu}(\mathbf{r}) \rangle \langle \chi^{(-)}(\mathbf{k}_c, \mathbf{R}_c) e^{i\alpha \mathbf{k}_v \cdot \mathbf{R}_c} | \chi^{(+)}(\mathbf{k}_a, \mathbf{R}_c) \rangle \\ &= \langle \mathbf{q}_v | V_{cv} | \Phi_a^{l\mu} \rangle \langle \chi^{(-)}(\mathbf{k}_c); \alpha \mathbf{k}_v | \chi^{(+)}(\mathbf{k}_a) \rangle . \end{aligned} \quad (6)$$

The momentum  $\mathbf{q}_v$  appearing in the first term is  $\mathbf{q}_v = \mathbf{k}_v - \gamma \mathbf{k}_a$ .

Here the structure information about the projectile is contained only in the first term, the vertex function, denoted by  $D(\mathbf{q}_v) = D_l(q_v) Y_{l\mu}(\hat{\mathbf{q}}_v)$ , where

$$D_l(q) = 4\pi \int_0^\infty dr r^2 j_l(qr) V_{cv}(r) u_l(r) . \quad (7)$$

The second factor is associated with the dynamics of the reaction only, which is expressible in terms of the bremsstrahlung integral [14].

The triple differential cross section for the elastic breakup reaction is

$$\frac{d^3\sigma}{dE_c d\Omega_c d\Omega_v} = \frac{2\pi}{\hbar v_a} \left\{ \frac{1}{2s_a + 1} \sum_{\sigma_c \sigma_v \sigma_a} |T_{\sigma_c \sigma_v \sigma_a}^{\text{AD}}|^2 \right\} \rho(E_c, \Omega_c, \Omega_v) , \quad (8)$$

or, upon carrying out the spin projection summations,

$$\frac{d^3\sigma}{dE_c d\Omega_c d\Omega_v} = \frac{2\pi}{\hbar v_a} \left\{ \sum_{l\mu} \frac{1}{(2l+1)} |\beta_{l\mu}^{\text{AD}}|^2 \right\} \rho(E_c, \Omega_c, \Omega_v) . \quad (9)$$

Here  $v_a$  is the  $a$ - $t$  relative velocity in the entrance channel. The phase space factor  $\rho(E_c, \Omega_c, \Omega_v)$  appropriate to the three-body final state is [15,16]

$$\rho(E_c, \Omega_c, \Omega_v) = \frac{h^{-6} m_t m_c m_v p_c p_v}{m_v + m_t - m_v \mathbf{p}_v \cdot (\mathbf{P} - \mathbf{p}_c) / p_v^2} \quad (10)$$

where, for the differential cross section in the laboratory frame,  $\mathbf{P}$ ,  $\mathbf{p}_c$  and  $\mathbf{p}_v$  are the total, core, and valence particle momenta in the laboratory system.

The core three dimensional momentum distribution  $\frac{d^2\sigma}{dp_c d\Omega_c}$  is related to its energy distribution cross section by

$$\frac{d^2\sigma}{dp_c d\Omega_c} = \sqrt{\frac{2E_c}{m_c}} \frac{d^2\sigma}{dE_c d\Omega_c} \quad (11)$$

$\frac{d^2\sigma}{dE_c d\Omega_c}$  can be readily obtained from the triple differential cross section above by integration with respect to the solid angle of the valence particle.

Both theoretically [17,18] and experimentally [19],  $^{11}\text{Be}$  is known to have a dominant  $1s_{\frac{1}{2}}$  neutron configuration in its ground state. We have calculated the breakup of  $^{11}\text{Be}$  assuming a  $1s_{\frac{1}{2}}$  neutron orbital with separation energy 0.504 MeV. The binding potential for  $^{11}\text{Be}$  is assumed to be of Woods-Saxon type with radius and diffuseness parameters 1.15 fm and 0.5 fm respectively. The depth of this potential has been calculated to reproduce the binding energy.

Very recently, the three dimensional momentum distribution  $\frac{d^2\sigma}{dp_c d\Omega_c}$  has been measured as a function of the momentum  $p_c$  of the  $^{10}\text{Be}$  core at MSU from elastic breakup of  $^{11}\text{Be}$  around 42 MeV/nucleon (41.71 MeV/nucleon) beam energy on a Au target at four different angles of  $0.64^\circ$ ,  $1.50^\circ$ ,  $2.88^\circ$  and  $4.39^\circ$  [11,20]. The fact that the target remains in the ground state has been ensured by observing no  $\gamma$ -rays in coincidence, which might result as a consequence of the de-excitation of the possibly excited target. The average momentum has been computed in each case.

We have calculated the momentum distributions of the  $^{10}\text{Be}$  fragment in the Coulomb breakup of  $^{11}\text{Be}$  on Au at 42 MeV/nucleon incident energy at these four angles. These have been shown in Fig. 2. The breakup of  $^{11}\text{Be}$  on high  $Z$  targets is known to be Coulomb dominated and this is even more true at forward angles [2,6,9,10]. Therefore, we have not considered nuclear contributions in our calculations. The average momentum at each angle has been calculated by using the expression  $\sum p_c \frac{d^2\sigma}{dp_c d\Omega_c} / \sum \frac{d^2\sigma}{dp_c d\Omega_c}$ . The post-acceleration should show up in the increase of this average momentum with increase of scattering angle. This is because with increase of scattering angle, the classical impact parameter decreases and the Coulomb repulsion on the outgoing charged fragment increases. In Fig. 3, we show results of our calculated average momenta along with calculations done for  $^{11}\text{Be}$  at 42 MeV/nucleon beam energy using methods of classical theory presented in [7]. With 42 MeV/nucleon incident energy, the beam velocity momentum is approximately 2806 MeV/c. Our calculated average momenta come around the same value. Therefore, we do not see any post-acceleration. The classical calculations, on the other hand, favour post-acceleration (Fig. 3). In our calculations, the Coulomb interactions in the final channel are included to all orders. It should be mentioned that higher order semi-classical theory in [21] and quantal theory with high energy approximation in [7] also did not support post-acceleration of  $^9\text{Li}$  in the breakup of  $^{11}\text{Li}$ . The experimental data, consistent with a constant average momentum over the range of scattering angles measured, also do not support the observation of this phenomenon. However, the experimentally deduced mean momenta (Fig. 3) are somewhat larger than 2797 MeV/c, which is the beam velocity momentum corresponding to the experimental beam energy of 41.71 MeV/nucleon.

In conclusion, our calculations on average momentum of the  $^{10}\text{Be}$  fragment at four different scattering angles following the Coulomb breakup of the one-neutron halo nucleus  $^{11}\text{Be}$  on a Au target at 42 MeV/nucleon beam energy gives no evidence of post-acceleration of  $^{10}\text{Be}$ . The calculations are performed within an approximate quantum mechanical theoretical model of elastic Coulomb breakup, which makes the following assumptions: (i) only the charged core interacts with the target via a point Coulomb interaction and (ii) that the important excitations of the projectile are to the low-energy continuum, and so can be treated adiabatically. The method permits a fully finite-range treatment of the projectile vertex and includes initial and final state interactions to all orders. The calculated results are compatible with the findings of recent good quality measurements at MSU. The results are consistent with a picture in which the breakup of  $^{11}\text{Be}$  takes place on a time-scale long compared to the collision time.

## ACKNOWLEDGMENTS

The author would like to thank Dr. J. A. Tostevin and Dr. I. J. Thompson of the University of Surrey, U.K. for stimulating discussions. Thanks are also due to Prof. R. Shyam for kindly going through this manuscript and making valuable suggestions.

## REFERENCES

- [1] H. Esbensen, G. F. Bertsch and C. A. Bertulani, Nucl. Phys. **A581**, 107 (1995).
- [2] P. Banerjee and R. Shyam, Nucl. Phys. **A561**, 112 (1993).
- [3] D. Sackett *et al.*, Phys. Rev. C **48**, 118 (1993); K. Ieki *et al.*, Phys. Rev. Lett. **70**, 730 (1993).
- [4] T. Nakamura *et al.*, Phys. Lett. **B331**, 296 (1994).
- [5] B. M. Sherrill, Nucl. Phys. **A583**, 725c (1995).
- [6] R. Anne *et al.*, Nucl. Phys. **A575**, 125 (1994).
- [7] G. Baur, C. A. Bertulani and D. M. Kalassa, Nucl. Phys. **A550**, 527 (1992).
- [8] T. Kido, K. Yabana and Y. Suzuki, Phys. Rev. **C50**, R1276 (1994).
- [9] P. Banerjee and R. Shyam, J. Phys. G **22**, L79 (1996).
- [10] P. Banerjee, I. J. Thompson and J. A. Tostevin, Phys. Rev. **C58**, 1042 (1998).
- [11] J. E. Bush *et al.*, Phys. Rev. Lett. **81**, 61 (1998).
- [12] J. A. Tostevin *et al.*, Phys. Lett. **B424**, 219 (1998); J. A. Tostevin, S. Rugmai and R. C. Johnson, Phys. Rev. **C57**, 3225 (1998).
- [13] R. C. Johnson, J. S. Al-Khalili and J. A. Tostevin, Phys. Rev. Lett. **79**, 2771 (1997).
- [14] A. Nordsieck, Phys. Rev. **93**, 785 (1954).
- [15] H. Fuchs, Nucl. Inst. and Meth. **200**, 361 (1982).
- [16] G. G. Ohlsen, Nucl. Inst. and Meth. **37**, 240 (1965).
- [17] F. M. Nunes, I. J. Thompson and R. C. Johnson, Nucl. Phys. **A596**, 171 (1996).
- [18] N. Vinh Mau, Nucl. Phys. **A592**, 33 (1995) and references cited therein.
- [19] B. Zwieglinski *et al.*, Nucl. Phys. **A315**, 124 (1979).
- [20] J. E. Bush, (University of Pennsylvania), private communications 1998.
- [21] S. Typel and G. Baur, Nucl. Phys. **A573**, 486 (1994).

FIGURES

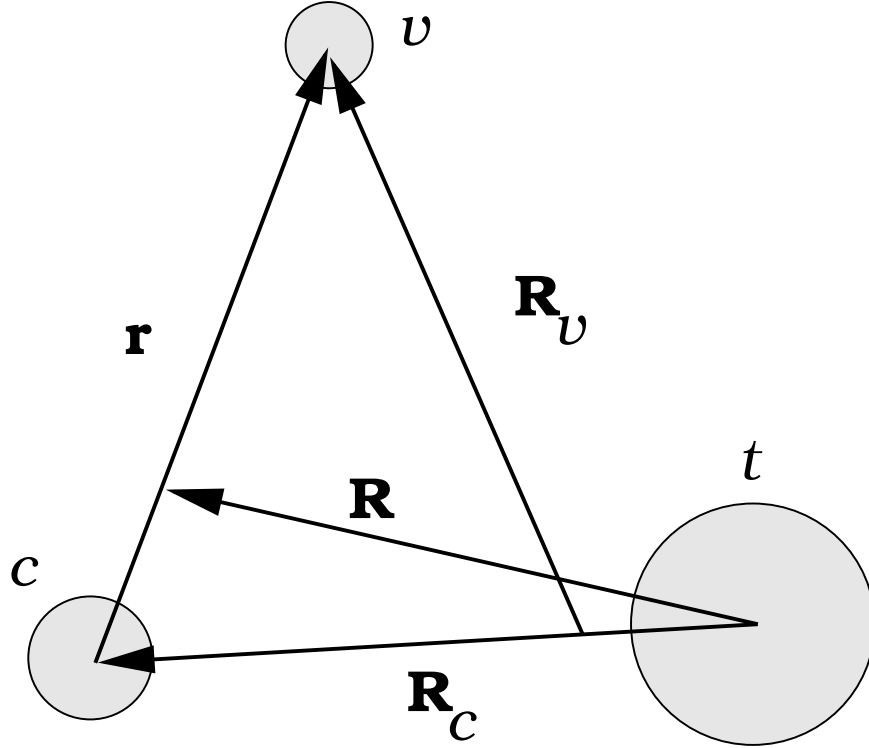


FIG. 1. Coordinate system adopted for the core, valence particle and target three-body system.

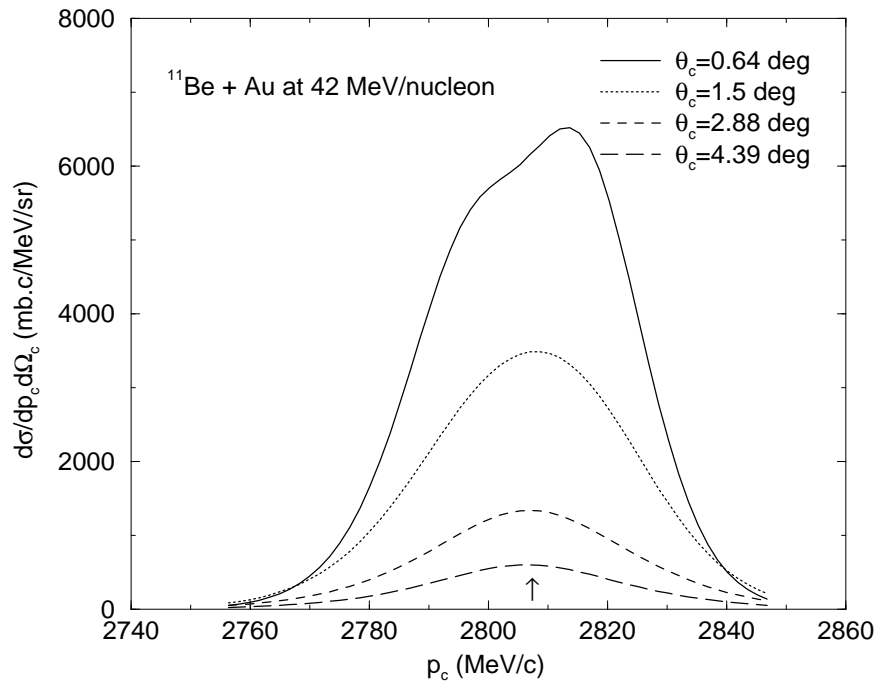


FIG. 2. Calculated three dimensional momentum distribution of  $^{10}\text{Be}$  from Coulomb breakup of  $^{11}\text{Be}$  on Au at 42 MeV/nucleon at four different laboratory angles of scattering of  $^{10}\text{Be}$ . The arrow on the horizontal axis indicates the position of the beam velocity momentum.



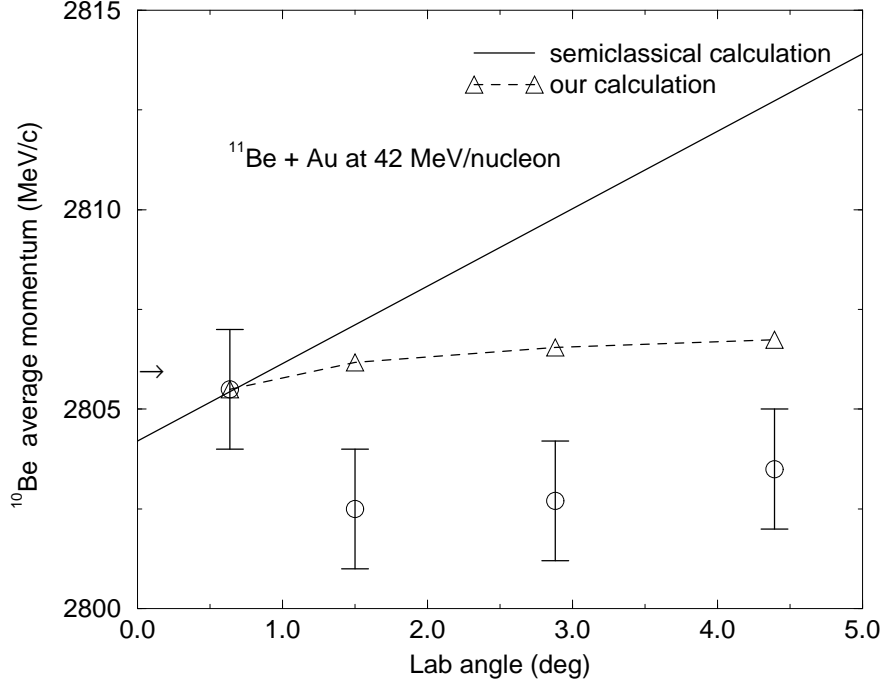


FIG. 3. Calculated average momentum of  $^{10}\text{Be}$  from Coulomb breakup of  $^{11}\text{Be}$  on Au at 42 MeV/nucleon as a function of the laboratory angle of scattering of  $^{10}\text{Be}$ . The experimental data, taken from [11], are at 41.71 MeV/nucleon. The semiclassical calculations are results of formulae in [7]. The arrow on the vertical axis indicates the position of the beam velocity momentum.